J|A|C|S ARTICLES

Published on Web 07/31/2009

Tuning Polymer Thickness: Synthesis and Scaling Theory of Homologous Series of Dendronized Polymers

Yifei Guo,[†] Jacco D. van Beek,[‡] Baozhong Zhang,[†] Martin Colussi,[†] Peter Walde,[†] Afang Zhang,*[,†] Martin Kröger,[†] Avraham Halperin,*[,§] and A. Dieter Schlüter*[,†]

Department of Materials, Institute of Polymers, Swiss Federal Institute of Technology, ETH Zurich, HCI J 541, 8093 Zurich, Switzerland, Department of Chemistry and Applied Biological Sciences, Swiss Federal Institute of Technology, ETH Zurich, 8093 Zurich, Switzerland, and Laboratoire de Spectrométrie Physique (LSP) CNRS Université Joseph Fourier, BP 87, 38402 Saint Martin d'Hères cedex, France

Received April 22, 2009; E-mail: afang.zhang@mat.ethz.ch; avraham.halperin@ujf-grenoble.fr; ads@mat.ethz.ch

Abstract: The thickness of dendronized polymers can be tuned by varying their generation *g* and the dendron functionality *X*. Systematic studies of this effect require (i) synthetic ability to produce large samples of high quality polymers with systematic variation of *g*, *X* and of the backbone polymerization degree *N*, (ii) a theoretical model relating the solvent swollen polymer diameter, *r*, and persistence length, λ, to *g* and *X*. This article presents an optimized synthetic method and a simple theoretical model. Our theory approach, based on the Boris-Rubinstein model of dendrimers predicts $r \sim n^{1/4}g^{1/2}$ and $\lambda \sim n^2$ where $n = [(X-1)^g - 1]/(X-2)$ is the number of monomers in a dendron. The average monomer concentration in the branched side chains of a dendronized polymer increases with *g* in qualitative contrast to bottle brushes whose side chains are linear. The stepwise, attach-to, synthesis of $X = 3$ dendronized polymers yielded gram amounts of $g = 1-4$ polymers with $N \approx 1000$ and $N \approx 7000$ as compared to earlier maxima of 0.1 g amounts and of $N \approx 1000$. The method can be modified to dendrons of different *X*. The conversion fraction at each attach-to step, as quantified by converting unreacted groups with UV labels, was 99.3% to 99.8%. Atomic force microscopy on mixed polymer samples allows to distinguish between chains of different *g* and suggests an apparent height difference of 0.85 nm per generation as well as an increase of persistence length with *g*. We suggest synthetic directions to allow confrontation with theory.

I. Introduction

Tuning the thickness of a polymer requires chemical modification of the backbone monomers, repeat units, by introducing substituents. Among the possible substituents, it is useful to distinguish between two extreme categories: Small groups such as phenyl or halide and side chains of different length and branching. The second category is of special interest because the number of monomers in the side chain, *n*, provides an adjustable tuning parameter of their thickness and persistence length. In other words, producing a homologous series of polymers that differ only in *n* allows studying the variation in thickness, persistence length and related physical properties as a function of *n*. From a chemistry point of view such polymers are of interest because they are endowed with a large number of end groups permitting control of solubility as well as further chemical modification. From a polymer physics perspective they afford the possibility of studying the scaling behavior with respect to *n* in addition to the familiar scaling behavior with respect to the backbone polymerization degree *N*. Among the side chains utilized, it is helpful to distinguish between two extremes: linear nonbranched chains producing "bottle brush" polymers[1] and regularly branched, dendron side chains leading to dendronized polymers (Figure 1).[2] This paper focuses on the second family. The main result reported in this article is the large scale synthesis of a homologous series of long dendronized polymers whose backbone monomers carry dendrons. To underline the polymer physics interest in the homologous series of dendronized polymers we first briefly discuss the theoretical scaling behavior of their thickness and persistence length with respect to *n*. The conformations of the polymers are characterized via analysis of their AFM images. This method permits fast data acquisition and analysis but introduces effects due to surface interactions and the preparation method.

[†] Department of Materials, Swiss Federal Institute of Technology.
[‡] Department of Chemistry and Applied Biosciences, Swiss Federal Institute of Technology.
[§] Université Joseph Fourier.

(1) For example, see: (a) Tsukahara, Y.; Namba, S. I.; Iwasa, J.; Nakano, Y.; Kaeriyama, K.; Takahashi, M. *Macromolecules* **2001**, *34*, 2624–2629. (b) Fischer, K.; Schmidt, M. *Macromol. Rapid Commun.* **2001**, *22*, 787–791. (c) Shinoda, H.; Miller, P. J.; Matyjaszewski, K. *Macromolecules* **2001**, *34*, 3186–3194. (d) Zhang, M.; Breiner, T.; Mori, H.; Müller, A. H. E. *Polymer* **2003**, *44*, 1449–1458. (e) Li, C.; Gunari, N.; Fischer, K.; Janshoff, A.; Schmidt, M. *Angew. Chem., Int. Ed.* **2004**, *43*, 1101–1104. (f) Bolisetty, S.; Airaud, C.; Xu, Y.; Mueller, A. H. E.; Harnau, L.; Rosenfeldt, S.; Lindner, P.; Ballauff, M. *Phys. Rev. E* **2007**, *75*, 040803.

(2) (a) Schlüter, A. D.; Rabe, J. P. *Angew. Chem., Int. Ed.* **2000**, *39*, 864–883. (b) Zhang, A.; Shu, L.; Bo, Z. S.; Schlüter, A. D. *Macromol. Chem. Phys.* **2003**, *204*, 328–339. (c) Frauenrath, H. *Prog. Polym. Sci.* **2005**, *30*, 325–384. (d) Schlüter, A. D. *Top. Curr. Chem.* **2005**, *245*, 151–191.

 © 2009 American Chemical Society

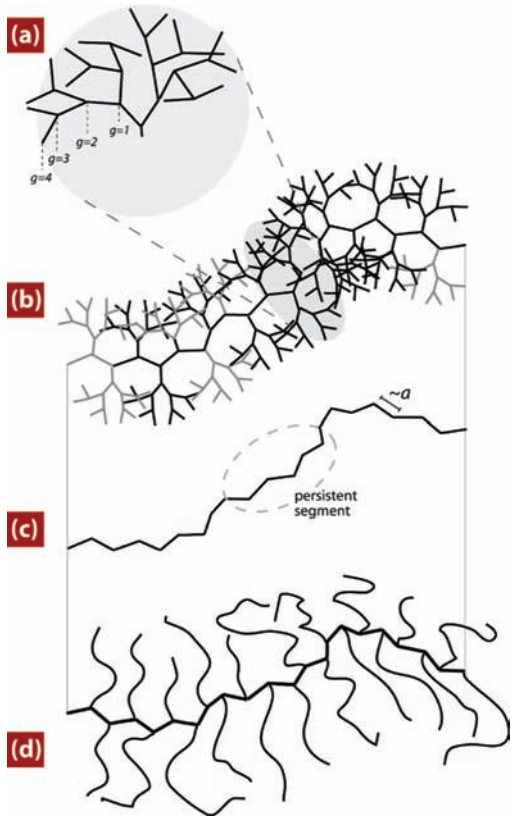

Figure 1. Dendronized polymers (b) vs bottle brushes (d). In both architectures the polymer comprises a semiflexible backbone (c) carrying side chains. The side chains in the dendronized polymers are repeatedly branched dendrons (a) while in the bottle brush the side chains are linear. For simplicity we depict dendrons comprising of monomers jointed by rigid rod like bonds.

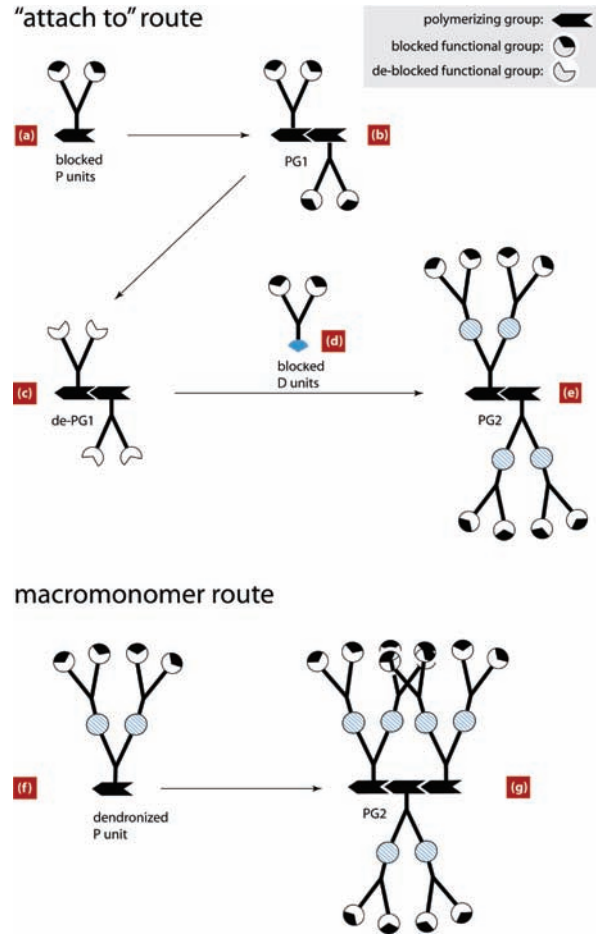

Figure 2. Synthetic Strategies: In the "attach to" route, P units carrying each two blocked functionalities (a) are polymerized thus forming a $g = 1$ dendronized polymer **PG1** (b). The resulting polymer is deblocked (c) and reacted with blocked D units (d) to yield a $g = 2$ dendronized polymer **PG2**. Higher generations are created by repeating steps (c) and (d). In the macromonomer route, the P units carry already a dendron of generation g ($g = 2$ in the figure) (f) and their polymerization leads directly to the dendronized polymer of this generation. Currently the macromonomer route does not allow to produce long dendronized polymers with $g > 2$ because the bulkiness of the P units (f) affects the polymerization reaction.

The combination of theory and synthesis is uncommon and requires comment. The synthetic method described affords the possibility of producing polymer samples comprising long chains of high quality and in gram amounts. It enables physics type experiments, involving for example scattering techniques, aiming to study the scaling behavior of dendronized polymers. This prospect poses questions of optimizing the polymer design to this end. The simple theoretical model proposed identifies physically relevant design parameters and their conformational effects. Combining these results with synthetic chemistry considerations suggests directions for future synthesis to better develop the study of the scaling behavior. Importantly, the theory also identifies distinctive problems associated with the study of such polymers and suggests a synthetic effort aimed to confront these questions. This point may be illustrated by considering the role of free ends. Dendronized polymers differ qualitatively from linear chains and bottle brushes in the importance of end effects. In linear chains comprising N monomers, end effects diminish as $1/N$ and are thus negligible for long chains. Their role is more important in bottle brushes where their importance diminishes as $1/n$. In marked distinction, free ends comprise more than 50% of the monomers in a dendronized polymer. Since their spatial distribution favors the exterior envelope of the chain, the free ends may dominate their solubility even if the "middle" monomers are poorly soluble. We return to this issue in more detail in sections II and III.

The thickness of dendronized polymers has a demonstrated effect on a variety of phenomena associated with such chains. Two examples illustrate this point. The first[3] is the increase of the fluorescence quantum yield of dendronized conjugated polymers with the generation number. In this case the dendrons afford the double advantage of solubilizing the backbone and preventing collisional quenching of its excited states. The second example concerns DNA adsorption onto oppositely charged, cationic dendronized polymers.[4] The DNA wraps the dendronized polymers forming a helix whose pitch decreases as the generation and the thickness increases.

The dendronized polymers were prepared using two types of trifunctional building blocks, polymerization (P) and dendronization (D) units (Figure 2). Both have two of the three functional groups blocked by protecting groups that can be removed or deprotected. The P unit, used for the creation of the polymer backbone carries a polymerizable methacrylate functionality. Upon polymerization of P one obtains a polymer, **PG1**, with every repeat unit carrying two protected function-

(3) Sato, T.; Jiang, D.-L.; Aida, T. *J. Am. Chem. Soc.* **1999**, *121*, 10658–10659.
(4) Gössl, I.; Shu, L. J.; Schlüter, A. D.; Rabe, J. P. *J. Am. Chem. Soc.* **2002**, *124*, 6860–6865.

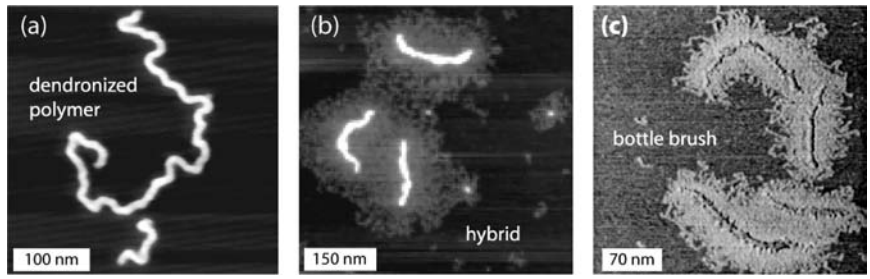

Figure 3. AFM images of $g = 4$ dendronized polymer (a), "hybrid" dendronized polymers ($g = 2$) where the terminal monomers of the dendrons carry linear chains ($n \approx 200$) forming an exterior bottle brush (b),[7] and bottle brush polymers with $n = 52$ attached to a "simple" polymer backbone (c).[8] The dendronized polymers in (a) and (b) appear as dense "sausages" while the linear side chains in (b) and (c) adsorb onto the surface thus forming a quasi two-dimensional brush.

alities. The protected functionalities of the polymer were then deprotected and reacted with D units having, in turn, two of their reactive functionalities blocked thus creating a second generation dendronized polymer **PG2**. The **PG2** polymer was then deprotected and reacted with unit D to create a third generation dendronized polymer **PG3** and upon further iteration fourth generation **PG4**. The following points merit attention: (i) The polymerization degree of the backbone, N, is kept constant[5] throughout the synthesis; (ii) In contrast to earlier work where the typical N range was $N \approx 200-400$[6] and the maximum value reported was $N \approx 1000$,[6e] in the present work $N \approx 1000$ and $N \approx 7000$ were attained; (iii) Identical D units were utilized at every step thus leading to true homologous series; (iv) At each stepwise addition 99.3−99.8% of the deprotected sites were successfully reacted with D units; (v) The synthetic route reported is optimized to produce gram amounts of dendronized polymers. Earlier work allowed to produce 0.1 g amounts[6] while in the present work the maximum attained was 8 g of **PG4** with $N \approx 1000$ and 1.5 and 0.7 g of **PG3** and **PG4** with $N \approx 7000$, respectively. In addition, it is important to note that the stepwise addition, "attach to" route, allows the production of long **PG3** and **PG4** polymers whereas the polymerization of dendronized monomers, the macromonomer route,[2b] only allows the production of short **PG3** and **PG4**.

As we shall discuss, the thickness of dendronized polymers allows to distinguish between species of different generation using Atomic Force Microscopy (AFM) (Figure 3). In contrast, it is clearly more difficult to discriminate between bottle brushes carrying side chains of different length (Figure 3). This is because the side chains are adsorbed and the individual side chains, with different positioning of their free ends, are discernible. "Polymer thickness" in these two systems assumes a different form. To rationalize these observed differences it is helpful to outline the theoretical description of three common manifestations of polymer thickness, in linear chains, bottle brushes and dendronized polymers. For simplicity we focus on polymer thickness as it applies to free chains in solution, when polymer-surface interactions do not play a role. This will allow us to qualitatively rationalize the AFM observations noted above. It also provides a basis for the quantitative interpretation of experiments concerned with the tunable thickness of dendronized polymers. Here we note that considerable effort was devoted to the theoretical description of dendrimers[9] and of bottle brushes.[10−14] In contrast, limited effort was devoted thus far to dendronized polymers.[15] Our discussion of this system utilizes approaches advanced for the study of dendrimers and of bottle brushes. In particular, we will utilize a Flory type model of dendronized polymers based on the Boris-Rubinstein[16] model for dendrimers combined with scaling arguments invoked in the discussion of persistence length of bottle brushes.[13] Using these methods we obtain the scaling behavior of the thickness, r, and persistence length, λ, of dendronized polymers with respect to g, the generation of the dendron and to the total number of monomers in the dendron, n. A simple version of the Flory model, overlooking the possible role of spacer chains, reveals three main conclusions: (i) As expected the "thickness" of dendrimers and of dendronized polymers exhibit slight differences in scaling behavior because the first are spherical objects while the second are locally cylindrical. Within the model we use the equilibrium thickness of dendronized polymers scales as $r_{eq} \sim n^{1/4}g^{1/2}$ while the dendrimer span scales as $r_{eq} \sim$

(5) The dendronization does not affect n but the chromatographic separations may introduce an n bias.

(6) For the step-by-step construction of higher generation dendronized polymers, see: (a) Shu, L.; Schäfer, A.; Schlüter, A. D. *Macromolecules* **2000**, *33*, 4321–4328. (b) Grayson, S. M.; Fréchet, J. M. J. *Macromolecules* **2001**, *34*, 6542–6544. (c) Zhang, A.; Vetter, S.; Schlüter, A. D. *Macromol. Chem. Phys.* **2001**, *202*, 3301–3315. (d) Shu, L.; Gössl, I.; Rabe, J. P.; Schlüter, A. D. *Macromol. Chem. Phys.* **2002**, *203*, 2540–2550. (e) Yoshida, M.; Fresco, Z. M.; Ohnishi, S.; Fréchet, J. M. J. *Macromolecules* **2005**, *38*, 334–344. (f) Al-Hellani, R.; Schlüter, A. D. *Helv. Chim. Acta* **2006**, *89*, 2745–2763. (g) Al-Hellani, R.; Barner, J.; Rabe, J. P.; Schlüter, A. D. *Chem.—Eur. J.* **2006**, *12*, 6542–6551. (h) Lee, C. C.; Fréchet, J. M. J. *Macromolecules* **2006**, *39*, 476–481. (i) Benhabbour, S. R.; Parrott, M. C.; Gratton, S. E. A.; Adronov, A. *Macromolecules* **2007**, *40*, 5678–5688. For the attachment of varyingly sized dendrons to non-dendronized backbones, see: (j) Desai, A.; Atkinson, N.; Rivera, F., Jr.; Devonport, W.; Rees, I.; Branz, S. E.; Hawker, C. J. *J. Polym. Sci., Part A: Polym. Chem.* **2000**, *38*, 1033–1044. (k) Helms, B.; Mynar, J. L.; Hawker, C. J.; Fréchet, J. M. J. *J. Am. Chem. Soc.* **2004**, *126*, 15020–15021. (l) Liu, Z.-T.; He, Y.-M.; Li, B.-L.; Liu, J.; Fan, Q.-H. *Macromol. Rapid Commun.* **2007**, *28*, 2249–2255.

(7) Zhang, A.; Barner, J.; Gössl, I.; Rabe, J. P.; Schlüter, A. D. *Angew. Chem., Int. Ed.* **2004**, *43*, 5185–5188.

(8) (a) Sheiko, S. S.; Prokhorova, S. A.; Beers, K. L.; Matyjaszewski, K.; Potemkin, I. I.; Khokhlov, A. R.; Möller, M. *Macromolecules* **2001**, *34*, 8354–8360. For reviews see: (b) Sheiko, S. S.; Möller, M. *Chem. Rev.* **2001**, *101*, 4099–4123. (c) Pyun, J.; Kowalewski, T.; Matyjaszewski, K. *Macromol. Rapid Commun.* **2003**, *24*, 1043–1059.

(9) Ballauff, M.; Likos, C. N. *Angew. Chem., Int. Ed.* **2004**, *43*, 2998.

(10) Birshtein, T. M.; Borisov, O. V.; Zhulina, E. B.; Khokhlov, A. R.; Yurasova, T. A. *Polym. Sci. USSR* **1987**, *29*, 1293.

(11) Zhulina, E. B.; Vilgis, T. A. *Macromolecules* **1995**, *28*, 1008–1015.

(12) Fredrickson, G. H. *Macromolecules* **1993**, *26*, 2825–2831.

(13) Potemkin, I. I.; Khokhlov, A. R.; Reineker, P. *Eur. Phys. J. E* **2001**, *4*, 93–101.

(14) Panyukov, S.; Zhulina, E. B.; Sheiko, S. S.; Randall, G. C.; Brock, J.; Rubinstein, M. *J. Phys. Chem. B* **2009**, *113*, 3750–3768.

(15) For a discussion of statistical properties of dendronized polymers under various solvent conditions, based on a lowest order virial expansion, see: Efthymiopoulos, P.; Vlahos, C.; Kosmas, M. *Macromolecules* **2009**, *42*, 1362–1369.

(16) Boris, D.; Rubinstein, M. *Macromolecules* **1996**, *29*, 7251–7260.

$n^{1/5}g^{2/5}$.[7,12] (ii) Bottle brushes and dendronized polymers are realizations of cylindrical brushes comprising side chain terminally attached to a backbone. In both cases the side chain stretch along the normal to the backbone in order to lower the monomer concentration and the associated interaction free energy. The competition between the elastic penalty and the interaction energy determines r_{eq}. For bottle brushes it leads to $r_{eq} \sim n^{3/4}$ while for dendronized polymers it results in $r_{eq} \sim n^{1/4}g^{1/2}$. While both r_{eq} increase with n, the n dependence of dendronized polymers r_{eq} is much weaker because their side chains are repeatedly branched. This leads to a qualitative difference in the n dependence of the average monomer volume fraction, ϕ_{eq}, $\phi_{eq} \sim n^{1/2}/g$ of dendronized polymers increases as g and n grow. In contrast ϕ_{eq} of bottle brushes decreases as $\phi_{eq} \sim n^{-1/2}$. Dendronized polymers thus occupy an intermediate position between linear chains and bottle brushes because their much higher density results in lower compressibility and deformability of the side chain corona. (iii) The persistence length of both bottle brushes and of dendronized polymers scales as $\lambda \sim n^2$.

We should emphasize that at present it is difficult to confront the theory with experimental results: (i) The theory, in its simplest form, applies to $g \geq 4$ polymers and a minimal comparison to scaling results requires a homologous series with $g = 4,5,6$. The applicability range can be extended by introducing long spacer chains. However, this requires a modification of the synthetic route. (ii) It is further necessary to characterize the quality of the different solvents in order to identify the Θ and good solvent regimes in terms of the corresponding virial coefficients. As noted earlier, this task is complicated by the high fraction of free ends in the dendronized polymers. As a result it is necessary to allow for interactions involving free ends, "middle" segments and the cross term (iii) to obtain theoretical estimates of the characteristics of a particular g it is necessary to obtain the dimensions of the side chain monomer.

In the following, we first discuss polymer thickness from a theoretical point of view. This discussion proceeds from the well studied cases of linear chains and bottle brushes to the poorly explored case of dendronized polymers. We then address the considerations motivating the choice of synthetic strategy for producing samples for physical exploration of thickness effects. Physics type experiments, such as the ones involving scattering techniques impose requirements in terms of sample size and polymer dimensions that limit the choice of synthetic methods. The synthesis used is then described, underlining the new features required to obtain gram amounts as well as the careful characterization of the final product and the intermediates.

II. Polymer Thickness from Linear Chains to Bottle Brushes and Dendronized Polymers - A Theoretical Perspective

Polymer thickness assumes different character as one moves from "simple" linear chains to polymers decorated by crowded side chains. The latter group includes polymers carrying side chains of different branching schemes. In the following we focus on the two extreme forms of branching: bottle brushes where the main chain monomers carry linear, nonbranched chains and dendronized polymers where the side chains are repeatedly branched dendrons (Figure 1). In the first group one may tune the polymer thickness and associated properties by modifying the backbone monomer structure with small substituents such as chloride or phenyl groups. This is exemplified by the different vinyl polymers obtained upon replacing one or more of the ethylene hydrogen by different atoms or groups for instance, polyvinyl alcohol, polystyrene and polyvinyl chloride. In the second group the primary control parameter is the number of monomers in the side chain, n. The boundary between these two approaches is not sharp and they are clearly indistinguishable when $n = 1$. However, for $n \gg 1$ the "side chain" approach leads to qualitatively different features. In the following we discuss these differences from the point of view of a simple Flory type theory. Our discussion aims to identify qualitative trends and their origins rather than to present a complete theoretical picture. We first recall the leading features of simple linear polymers which serve as reference case for our discussion of thickness and its consequences.

The theoretical description of large scale polymer behavior does not incorporate explicitly the detailed molecular structure of the chains. Rather the molecular structure is absorbed into two coarse grained parameters. One is the monomer diameter, a, that accounts for the "thickness" of a linear polymer chain. The second parameter, l_p, allows for chain rigidification due to hindered rotation. It gives rise to persistent rodlike segments, comprising $p > 1$ monomers and thus having a length of roughly $l_p \approx pa$. The diameter a and persistence length l_p are correlated since the potential barrier to rotation increases upon introduction of bulky side groups. This is evident from empirical observations and their rationalization by the rotational isomeric state model.[17] While a is related to the monomer structure and reflects bond lengths, angles and the bulkiness of the side groups attached, it is typically considered as a phenomenological parameter. In particular a is determined from the specific volume per persistence length l_p. Importantly, a is considered as a monomeric property that is weakly affected by the composition and the sequence of a copolymer chain. This is in contrast, as we shall discuss later, to the thickness of polymers carrying side chains which is strongly dependent on the side chain crowding induced by the polymerization.

The effects of a and p on polymer behavior are illustrated by their role in the Flory type description of semiflexible chains with $p > 1$.[18] When p is much smaller than the polymerization degree N, $N \gg p > 1$, the chain can be viewed as a coil comprising N/p persistent segments. This affects three aspects of the chain behavior as discussed within a Flory type theory aiming to obtain the chain's span R. First, the elastic free energy, $F_{el}/k_BT \approx (R/R_0)^2$ is weakened because the radius of a random walk of persistent segments is larger $R_0/a \approx (N/p)^{1/2}p = (Np)^{1/2} > N^{1/2}$. Second, two mutually canceling changes occur in the interaction free energy $F_{int}/k_BT \approx vc^2R^3$ where $c = \phi/a^3$ is the monomer concentration within the coil, ϕ is the corresponding volume fraction and v is the virial coefficient of binary monomer−monomer interactions. Viewing the two interacting persistent segments as cylinders leads, following Onsager theory, to a second virial coefficient $v \approx l_p^2a\tau = p^2a^3\tau$ instead of $v \approx a^3\tau$ for a flexible chain of spherical monomers. Here $\tau = (T - \Theta)/T$ is the reduced temperature defined in terms of the Θ temperature. On the other hand, the monomer concentration $c = N/R^3$ is replaced by the concentration of persistent segments N/pR^3. As a result, the Flory radius of a persistent chain, when $F_{el} \approx F_{int}$, is $R_F \approx (p\tau)^{1/5}N^{3/5}a$ rather than $R_F \approx \tau^{1/5}N^{3/5}a$. Two additional effects are of greater importance. One is the appearance of a marginal solvent regime for $p > 1$. In this regime,

(17) Flory, P. J. *Statistical Mechanics of Chain Molecules*; John Wiley: New York, 1969.
(18) Schaefer, D. W.; Joanny, J. F.; Pincus, P. *Macromolecules* **1980**, *13*, 1280–1289.

occurring roughly at $\tau \geq \phi \geq \tau/p^3$, the chains are Gaussian and the osmotic pressure scales as ϕ^2. In contrast the osmotic pressure of semidilute polymer solutions in a Θ solvent and in a good solvent scales respectively as ϕ^3 and $\phi^{9/4}$.[15,16] Second, liquid crystalline order can occur when $p \gg 1$.[19]

As noted above, tuning a and l_p is possible by chemically introducing bulkier substituents into the monomer so as to increase the potential barriers for rotation around monomer−monomer bonds. When this approach works, it affords a powerful and cost-effective method. Its scope is however limited for the following two reasons: (i) While the general trend is that bulkier side groups rigidify the linear chain, as illustrated for example by polystyrene, there are exceptions to the rule such polyethylene whose persistence length is high in spite of the absence of bulky substituents;[20] (ii) Chemical modification can strongly affect the solubility of the polymer.

Tuning the thickness and persistence length by introducing side chains incorporating n monomers is an alternative strategy. As noted earlier, the boundary between the two is fuzzy for small n. Yet, for $n \gg 1$ the side chain effect on the polymer thickness and the persistence length changes qualitatively. To underline this distinction we denote the "side chain" thickness by r and the corresponding persistence length by λ. While the effects of r and λ are similar to those of a and l_p, as discussed above, four points merit emphasis: (i) r is no longer a monomeric quality since it reflects the stretched conformations of the crowded side chains thus becoming a chain attribute. (ii) While "normal" monomers are impenetrable, a polymer decorated by side chains can accommodate solvent and solutes within its diameter r. Furthermore, r in contrast to a will be modified by compression and the interactions between different chain segments are not expected to exhibit hard core repulsion at separations smaller than r. In effect, the "hard thickness" of simple chains is replaced by "soft thickness" for polymers carrying side chains. (iii) The variation of r and λ with n for $n \gg 1$ becomes systematic while the effect on the solubility is weakened thus permitting rational design. (iv) The theoretical description of r involves the statistical physics of the flexible side chains rather than the quantum chemistry of the backbone monomers. Accordingly, the equilibrium thickness r_{eq} is determined by minimization of the appropriate free energy.

To illustrate the flavor of the polymer thickness as tuned by n of the side chains we consider bottle brushes and dendronized polymers using a Flory type theory. We first discuss the well established case of bottle brushes and then modify the description to the case of dendronized polymers. In both cases an important control parameter is the number of backbone monomers m between monomers carrying side chains. For brevity we limit the discussion to the range $1 \leq m \leq p$ when the spatial separation between the anchoring sites of side chains, δ, is fixed and does not vary with the crowding. For $m \geq p$ it is necessary to allow for the extension of the chain segments separating the grafting sites.[10] In addition, we restrict our analysis to the limit of λ much larger than l_p of the backbone thus assuring a cylindrical local symmetry.

II.a. Bottle Brushes. The Flory type theory of bottle brushes introduces two assumptions (i) the linear side chains are uniformly stretched with their ends straddling the brush boundary at r. (ii) The associated monomer concentration profile is step like with a constant monomer concentration of $n/r^2\delta$. The Flory free energy per side chain is

$$\frac{F}{k_BT} \approx \frac{r^2}{r_0^2} + \frac{\upsilon n^2}{r^2\delta} \tag{1}$$

where υ is the second virial coefficient and $r_0 \approx n^{1/2}a$ is the span of an ideal side chain. The first term specifies the Gaussian elastic free energy of a flexible side chain extended beyond r_0. The second term accounts for its interaction free energy due to binary interactions of the side chain monomers with a "monomer cloud" having a concentration of $n/r^2\delta$. Here we focus on the limit of strongly crowded and long side chains in a good solvent where additional terms, allowing for ternary interactions and folding back of the ends, are negligible. Minimization with respect to r yields the equilibrium condition when the elastic term and the interaction penalty are comparable. This determines the equilibrium span of the side chains r_{eq},

$$r_{eq} \approx \left(\frac{\upsilon}{a^3}\right)^{1/4}\left(\frac{a}{\delta}\right)^{1/4} n^{3/4}a \tag{2}$$

thus specifying the equilibrium monomer volume fraction

$$\phi_{eq} \approx \frac{na^3}{r_{eq}^2\delta} \approx \frac{1}{n^{1/2}}\left(\frac{a}{\delta}\right)^{1/2}\left(\frac{a^3}{\upsilon}\right)^{1/2} \tag{3}$$

Upon substitution of r_{eq} in F (eq 1), one obtains the equilibrium free energy per unit length

$$\frac{F_{eq}}{\delta k_BT} \approx \frac{1}{a}\left(\frac{\upsilon}{a^3}\right)^{1/2}\left(\frac{a}{\delta}\right)^{3/2} n^{1/2} \tag{4}$$

With F_{eq}/δ and r_{eq} at hand we may estimate the persistence length owing to the bottle brush using a scaling argument due to Birshtein et al.[10,11,13] For an infinite bottle brush, the only energy density scale is F_{eq}/δ and the only length scale is r_{eq}. Accordingly the free energy per unit length of a uniformly bent rod with radius of curvature ρ is

$$\frac{F_{rod}}{k_BT} \approx \frac{F_{eq}}{\delta k_BT}\left[1 + \left(\frac{r_{eq}}{\rho}\right)^2\right] \tag{5}$$

This form is obtained by expanding F_{rod} in powers of r/ρ and retaining the first non vanishing term, assuming that the bottle brush has no spontaneous curvature thus imposing the absence of a term linear in r/ρ. Comparison to the bending free energy density of a persistent chain, $F_{bend} \approx k_BT\lambda/\rho^2$,[21] then yields

$$\lambda \approx \frac{F_{eq}}{\delta k_BT} r_{eq}^2 \approx \frac{\upsilon}{a^3}\left(\frac{a}{\delta}\right)^2 n^2 a \tag{6}$$

The scaling behavior of λ as obtained above is appropriate to polymers under marginal solvent conditions. In a good solvent the Flory free energy yields the correct r_{eq} but overestimates F_{eq}. Accordingly, λ obtained for such conditions via blob arguments, allowing for correlation effects neglected in the Flory approach, exhibits a slightly weaker n dependence. Further differences occur when the backbone is allowed to stretch so as to lower the crowding of the side chains. Finally, note that

(19) Grosberg, A. U.; Khokhlov, A. R. *Statistical Physics of Macromolecules*; AIP Series in Polymers and Complex Materials: New York, 1994.

(20) Rubinstein, M.; Colby R. H. *Polymer Physics*; Oxford University Press: Cambridge, 2003.

(21) Odijk, T. *J. Polym. Sci. Polym. Phys. Ed* **1977**, *15*, 477–483.

eq 6 describes the polymer rigidity when the side chain contribution is dominant. Current experiments suggest that $n > 30$ is necessary to reach this regime.[22]

II.b. Dendronized Polymers. We now turn from bottle brushes, where the side chains are linear, to dendronized polymers carrying repeatedly branched side chains. For simplicity we first consider the case of dendrons comprising of monomers attached by rigid freely jointed bonds of length a. The dendrons are characterized by two chemical design parameters. One is the functionality of the monomers forming the junctions, X. The second is the generation of the dendron, g, which counts the number of monomers in a strand joining the origin and a free end. In chemistry terms $g - 1$ is the number of deblocking steps in the synthesis. The currently experimentally attainable values are $X \leq 6$ and $g \leq 5$. For the formulation of theory it is convenient to use g and $n = [(X - 1)^{g-1}]/(X - 2)$ instead of g and X. The implementation of the Flory approach to dendrimers is less obvious in comparison to the bottle brushes. This is because of the difficulty in characterizing the elastic free energy of repeatedly branched chains. To this end we follow Boris and Rubinstein[16] and consider the free energy of a linear strand comprising g monomers joining the origin and a terminal group and having a Gaussian span of $r_0 \approx g^{1/2}a$. As before our analysis concerns a locally cylindrical chain with crowded dendrons, $\delta < r_0$, leading to a Flory free energy per *strand* of

$$\frac{F_{\text{strand}}}{k_B T} \approx \frac{r^2}{r_0^2} + \frac{\upsilon n g}{r^2 \delta} \tag{7}$$

This free energy differs from 1 in two respects. First, $r_0 \approx g^{1/2}a$ replaces $r_0 \approx n^{1/2}a$ and the elastic penalty is thus controlled by g. Second, while the interaction free energy per monomer remains $\upsilon n/r^2\delta$ the interaction free energy per strand becomes $\upsilon g n/r^2\delta$. The equilibrium condition $\partial F/\partial r = 0$, when the two terms are comparable, leads to

$$r_{\text{eq}} \approx \left(\frac{\upsilon}{a^3}\right)^{1/4}\left(\frac{a}{\delta}\right)^{1/4} n^{1/4} g^{1/2} a \tag{8}$$

and

$$\phi_{\text{eq}} \approx \frac{n a^3}{r_{\text{eq}}^2 \delta} \approx \left(\frac{a^3}{\upsilon}\right)^{1/2}\left(\frac{a}{\delta}\right)^{1/2} \frac{n^{1/2}}{g} \tag{9}$$

Upon substituting r_{eq} in F_{strand}, eq 7, one obtains the equilibrium free energy per strand F_{eq}. However, in order to estimate the persistence length λ we need the equilibrium free energy per dendron. Since a strand comprises g monomers while a dendron consists of n monomers, the equilibrium free energy per dendron is n/g larger. Accordingly the free energy density specifying λ is

$$\frac{n F_{\text{eq}}}{g \delta k_B T} \approx \frac{1}{a}\left(\frac{\upsilon}{a^3}\right)^{1/2}\left(\frac{a}{\delta}\right)^{3/2} \frac{n^{3/2}}{g} \tag{10}$$

leading, using eq 5 as introduced earlier, to

$$\lambda \approx \frac{n F_{\text{eq}}}{g \delta k_B T} r_{eq}^2 \approx \frac{\upsilon}{a^3}\left(\frac{a}{\delta}\right)^2 n^2 a \tag{11}$$

The free energy 7 considers free ends and "middle" monomers as identical. We focus on this simplest situation for brevity and because it does allow to confront computer simulations. In view of the large number of free ends a more realistic treatment should distinguish between three different interactions: free end−free end, middle monomer−middle monomer as well as middle monomer−free end. These are associated with four different virial coefficients, υ_{ee}, υ_{em}, υ_{me} and υ_{mm}. Upon denoting the number of free ends by n_e the interaction term $\upsilon n g/r^2\delta$ should then be replaced by $[\upsilon_{ee}(n_e - 1) + \upsilon_{em}(n - n_e) + \upsilon_{me}(g - 1)\, n_e + \upsilon_{mm}(n - n_e)(g - 1)]/r^2\delta$. One may further envision the case that the middle monomers or the free ends experience Θ or poor solvent conditions thus requiring the introduction of ternary interactions terms. Such analysis is beyond the scope of this paper, especially since the virial coefficients, υ_{ee}, υ_{em}, υ_{me} and υ_{mm} are currently unknown. Importantly, the second virial coefficient of a dendronized polymer will reflect the overall interactions between repeat units of the polymer and will not specify υ_{ee}, υ_{em}, υ_{me} and υ_{mm}. On the other hand, a rough estimate of υ_{mm} and υ_{ee} may be obtained from the solution properties of linear polymers comprising of bifunctional variants of the D units and P units. We address the synthetic issues involved in section III.

We should emphasize two additional reservations concerning our discussion of dendronized polymers. First, while the shortcomings of the Flory approach are well understood for linear chains its performance for dendrons received less attention. Second, for brevity we focused on dendrons whose junctions are joined by freely jointed rigid bonds thus ignoring the possible role of flexible spacers.

II.c. Bottle Brushes vs Dendronized Polymers. The number of free ends per grafting site, n_e, as well as the key physical attributes of dendronized polymers and bottle brushes, as obtained from the Flory type theory we utilized, are summarized in Table 1.

In both systems, r_{eq} and λ are tunable and reflect the size and the crowding of the side chains. Yet, the branching of the dendron side chains makes for smaller r_{eq} and higher ϕ_{eq}. Thus r_{eq} of a dendronized polymer with $X \geq 3$ is smaller by a factor of $(g/n)^{1/2} < 1$ where $n = [(X - 1)^g - 1]/(X - 2)$, while their average monomer volume fraction ϕ_{eq} is larger by a factor of n/g. Since r_{eq} scales as $\sim n^{1/4}g^{1/2}$ while n scales as $\sim(X - 1)^g$, both $r_{\text{eq}}(n)$ and $r_{\text{eq}}(g)$ curves depend strongly on X (Figure 4). $r_{\text{eq}}(g)$ of bottle brushes, where $n = g$, is steeper than $r_{\text{eq}}(g)$ of dendronized polymers with $X \geq 3$. This is associated with a qualitative effect on ϕ_{eq}. For bottle brushes ϕ_{eq} decreases with $n = g$ while for dendronized polymers it is an increasing function of g. The different ϕ_{eq} suggest corresponding differences in penetrability and compressibility. For example, the attainable maximal g corresponding to $\phi_{\text{eq}} = 1$ is $g_{\max} \approx n^{1/2}(a/\delta)^{1/2}$ arising because the volume occupied by the dendron is roughly na^3 while the maximal available volume is $g^2a^2\delta$. There is no corresponding effect for bottle brushes. On the other hand, within our Flory type analysis, the persistence length λ of the two polymer families is identical. This is because the characteristic free energy density we utilize assumes the form $n^2kT/\delta^2 r_{\text{eq}}^2$ for both systems. Another important difference concerns the number of free ends, n_e. This affects, of course, the number of reactive groups available for further chemistry. However, it also plays a role in the theoretical description of

(22) Zhang, B.; Gröhn, F.; Pedersen, J. S.; Fischer, K.; Schmidt, M. *Macromolecules* **2006**, *39*, 8440–8450.

(23) The configurations of long dendronized polymers can be deduced from scattering in the range $1/R_g \ll q \ll 1/\lambda$ where q is the amplitude of the scattering vector. In this range the scattered intensity scales as q^{-D} where D is the fractal dimension of the polymer.[18] The $L \geq 10\lambda$ requirement is a lower bound on the necessary q range.

Table 1. Dendronized Polymers vs Bottle Brushes: Number of Free Ends Per Grafting Site, n_e, Equilibrium Span of the Side Chain, r_{eq}, Equilibrium Monomer Volume Fraction, ϕ_{eq}, and Persistence Length λ[a]

	n_e	r_{eq}/a	ϕ_{eq}	λ/a
Dendronized polymers	$(X-1)^{g-1}$	$(v/a^3)^{1/4}(a/\delta)^{1/4}n^{1/4}g^{1/2}$	$(a^3/v)^{1/2}(a/\delta)^{1/2}n^{1/2}/g$	$(v/a^3)(a/\delta)^2n^2$
Bottle brushes	1	$(v/a^3)^{1/4}(a/\delta)^{1/4}n^{3/4}$	$(a^3/v)^{1/2}(a/\delta)^{1/2}n^{1/2}$	$(v/a^3)(a/\delta)^2n^2$

[a] The expressions correspond to the case of dendrons comprising monomers jointed by rigid bonds of length a ignoring the effect of flexible spacers, addressed briefly later in the text.

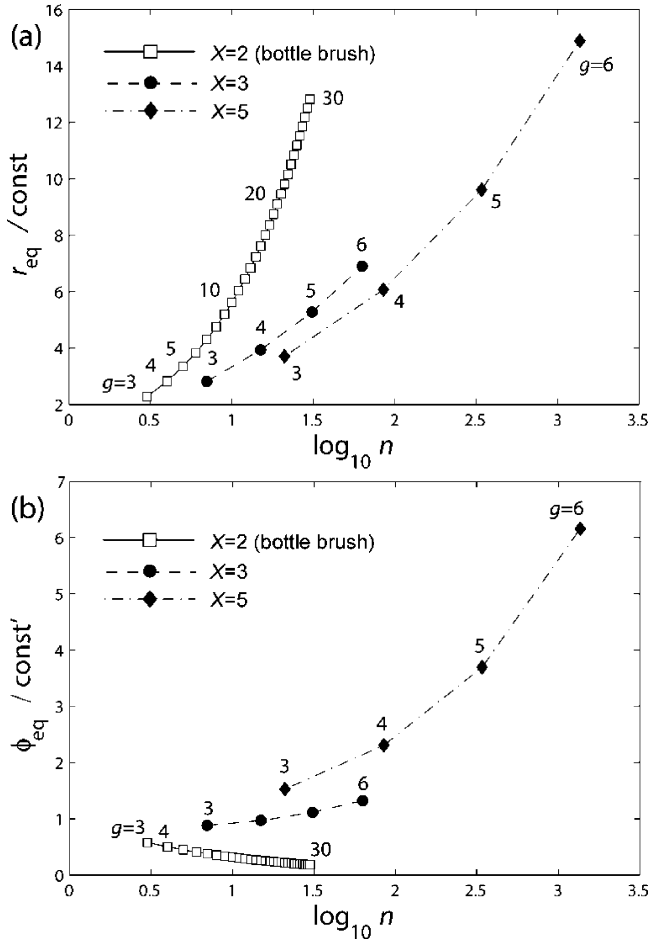

Figure 4. (a) Plots of $n^{1/4}g^{1/2} \approx r_{eq}$/constant of dendronized polymers and $n^{3/4} \approx r_{eq}$/constant of bottle brushes vs $\log_{10}(n)$ for different junction functionalities X. For bottle brushes with $X = 2$, $g = n$ while for $X > 2$, $n = [(X-1)^{g-1}]/(X-2)$. Increasing the junction functionality X results in a much wider range of n and r_{eq}. (b) Plots of $n^{1/2}/g \approx \phi_{eq}$/constant of dendronized polymers and $n^{-1/2} \approx \phi_{eq}$/constant of bottle brushes. The average density of bottle brushes decreases with $g = n$ while dendronized polymers exhibit the opposite trend.

the systems. Our highly simplified approach does not distinguish between end groups and "interior monomers" thus ignoring end effects. This is reasonable for bottle brushes, where $n_e/n = 1/n$, when n is large enough. It is never reasonable in the case of dendronized polymers where n_e/n is of order unity since $n_e/n \geq (X-2)/(X-1) \geq 1/2$. Accordingly, a more realistic Flory free energy should distinguish between monomer−monomer, end−end and end−monomer interactions. Note that in our simplified discussion, bottle brushes constitute a special case of dendronized chains. All the quantities n_e, r_{eq}, ϕ_{eq}, and λ of dendronized polymers reduce to the bottle brush form when $X = 2$ leading, upon invoking L'Hôpital's rule to evaluate $n = [(X-1)^g - 1]/(X-2)$, to $n = g$.

The simple picture presented above was attained at a price of overlooking many refinements of possible importance, especially for confronting theory with experiment. Some of the missing points are briefly discussed below, beginning with the bottle brush results. The Flory approximation as presented earlier considers flexible side chains in a good solvent. In this regime this approximation yields the correct r_{eq} and average ϕ_{eq} but overestimates F_{eq}. The Flory approximation will yield the correct scaling forms for the marginal solvent regime of semiflexible chains with $p > 1$. In this case r_{eq}/a is larger by $p^{1/4}$ while ϕ_{eq} and F_{eq} are smaller by a factor of $p^{-1/2}$. These effects cancel in $\lambda \approx r_{eq}^2F_{eq}/(\delta k_BT)$ which remains unmodified. In a good solvent it is necessary to allow for correlations due to self-avoidance of the chains. This can be done using blob arguments. For cylindrical brushes of flexible chains the blob picture yields, as we discussed, an identical $r_{eq} \approx (a/\delta)^{1/4}n^{3/4}$ but a lower $F_{eq} \approx (a/\delta)^{5/8}n^{3/8}$. It leads accordingly to[9] $\lambda \approx (a/\delta)^{17/8}n^{15/8}$ instead of $\lambda \approx (a/\delta)^2n^2$ as obtained from the Flory approximation. Note that within the blob picture the monomer concentration profile decreases with r as $\phi \approx r^{-2/3}$ in contrast to the step-like concentration profile, $\phi \approx r^0$, assumed in the Flory approximation.[10] The results cited above, as in our earlier discussion, assume a non extendable backbone. A somewhat different scaling behavior is obtained for $m > p$, when the extension of the backbone should be taken into account.[10]

Our discussion of the dendronized polymers did not allow for the role of spacer chains between the junctions. A simple discussion of this effect is possible, along the lines proposed by Boris and Rubinstein,[16] by considering a dendron such that each junction is attached to its predecessor by a flexible spacer comprising s monomers of size b. For simplicity there is no distinction between the junction monomers and spacer monomers and all binary interactions are characterized by the same virial coefficient v. In this approach a is replaced by $s^{1/2}b$ thus leading to $r_0 \approx (gs)^{1/2}b$ instead of $r_0 \approx g^{1/2}a$. The interaction term $vng/(r^2\delta)$ becomes $vs^2ng/(r^2\delta)$. Altogether, the introduction of spacers lowers the elastic free energy by a factor of s^{-1} while increasing the interaction energy by a factor of s^2. It gives rise to stronger stretching of the side chains $r_{eq}/b \approx (v/b^3)^{1/4}(b/\delta)^{1/4}s^{3/4}n^{1/4}g^{1/2}$ and thus to a lower monomer volume fraction $\phi_{eq} \approx nsb^3/(r_{eq}^2\delta) = (b^3/v)^{1/2}(b/\delta)^{1/2}(n/s)^{1/2}/g$. The equilibrium free energy per dendron is also higher $F_{eq}/k_BT \approx (v/b^3)^{1/2}(b/\delta)^{1/2}s^{1/2}n^{1/2}$ leading to a persistence length $\lambda \approx nF_{eq}r_{eq}^2/(g\delta k_BT)$ or $\lambda \approx (v/b^3)(b/\delta)^2s^2n^2b$. Note that the separation of a strand into junctions and spacers is somewhat arbitrary and different virial coefficients may be actually necessary to describe junction−junction, junction−spacer and spacer−spacer interactions.

The above results for the persistence length assume that $\lambda \gg l_p$ and that the chain rigidity is dominated by the side chain interactions. The precise boundary of this regime is not well established. Recent experimental results concerning the persistence length of bottle brush polymers with $6 \geq n \geq 33$ did not follow a power law behavior predicted by any of the bottle brush models. Rather, they suggested that the effective persistence length l_{eff} behaves as $l_{eff} = l_p + \lambda(n)$ and that this n range corresponds to a cross over between backbone dominated regime and the side chain domination regime.[22] Experimental study of the scaling behavior of r and λ requires samples spanning a

wide range of g and n values. Since the currently accessible range of g is limited to $g \leq 5$, this goal can be attained by variation of the functionality X thus allowing to explore a wide range of $n \gg 1$ between $n(X = 6,g = 5) = 781$ and $n(X = 3,g = 5) = 31$. In implementing this approach it is desirable to minimize the structural differences between junction monomers of different X.

III. Synthesis of Homologous Series

III.a. Conceptual Considerations. To systematically explore the properties of homologous series of dendronized polymers aiming at unraveling potential thickness effects, its representatives must (i) have sufficiently long backbone chains, (ii) have high structural fidelity, and (iii) be available in gram quantity. These conditions fundamentally affect the kind of chemistry to be used for their synthesis as will become evident from the following considerations. With regard to scattering experiments it is useful to distinguish between two situations: Polymers whose contour length L is comparable to the persistence length λ and those with $L \gg \lambda$. Polymers with $L \approx \lambda \gg r_{eq}$ are expected to behave as bendable rods while long polymers with $L \gg \lambda$ will behave as coils of L/λ segments of length λ each. In practice $L/\lambda \geq 10$ is necessary for scattering experiments aiming at this last regime.[21] Current results suggest that λ of **PG4** is in the range $10 - 50$ nm.[24] Accordingly, the $L \approx 10\lambda$ criterion requires polymers of length of several hundred nanometers up to a micrometer. This condition rules out the use of the by far most often used synthesis method, the so-called macromonomer route (Figure 2),[2b] in which macromonomers already carrying the dendrons of final size are polymerized. Even with the recent improvement of the number average degrees of polymerization, P_n, in the polymerization of macromonomers under supercriticial carbon dioxide high pressure conditions,[25] $L > 500$ nm and $L > 40$ nm are presently unrealistic for $g = 3$ and $g = 4$ polymers, respectively. The attach-to route was therefore the only option for $g = 4$ polymers with $L \approx 10\lambda$. It suggested itself strongly also for $g = 3$ polymers inasmuch as flask-type chemistry under ambient conditions was preferable to synthesis under high pressure.[26] In this method the dendronized polymers are obtained in a step-by-step process in which generation after generation is added to an already existing starting polymer (Figure 2); thousands of reactions have to be performed with each individual polymer chain. This immediately raises the issue of structural fidelity, that is, the conversion fraction per dendronization step. Though structural fidelity was not normally addressed in a quantitative manner in the pertinent literature, there is a precedent that such procedures can in fact be carried out in high level of conversion.[27] It was therefore a natural choice to use this approach, with all its particular chemistry, in the present case.

The step-by-step process also raises the question as to whether the length of the starting polymer (**PG1**) has an impact on the structural fidelity especially for the synthesis of high generation polymers. This is an issue that has not yet been addressed quantitatively in the literature, but it is useful to note that all starting polymers used so far for which quantitative experiments are reported have short chains with $P_n \leq 400$, thus much shorter than the target of the present work. There is the one exception with $P_n = 1100$ and $P_w = 1300$.[6e,28] Obviously new grounds had to be explored in regard to how, polymer chains with, for example, $P_n \approx 7000$ and weight average degrees of polymerization $P_w \approx 13\,000$ behave in consecutive dendronization reactions. Finally, the aspect of quantity needs to be addressed. Typically, attach-to experiments are performed on a scale that allows doing the final steps (**PG3** to **PG4**) with a few tenths of a milligram material.[6] Sometimes the amounts obtained are not even stated, which may indicate that they are rather small. For studying polymer thickness effects, milligram quantities are inadequate. It is thus important to establish a protocol enabling the synthesis of each member of a homologous series at least on the gram scale. All these considerations led us to devise the route in Scheme 1.

The advantages of this strategy are manifold. Monomer **MG1** and the two polymers **PG1** and **PG2** are known from earlier work which facilitates their characterization.[29] Also the deprotection chemistry, using neat trifluoroacetic acid, has been employed numerous times and found to be highly reliable.[30] The key building block for dendronization, compound **1** (Scheme 1), is new. However, its synthesis rests upon a commercially available dendrons, **2a** and **2b**. Furthermore the way it bonds to peripheral amines during the dendronization event, succinidyl active ester amidation, has been quantified in the few similar cases mentioned above. Under carefully optimized conditions, coverages of up to 99.8% were reproducibly achieved[6d] which obviously suggested this building block for the present purpose. Finally, monomer **MG1** can be polymerized by controlled or, alternatively, free radical polymerization. This allowed obtaining starting polymers **PG1** with different chain lengths in the range of several hundred nanometers.

Considering the enormous increase in molar mass during the homologization which may also be referred to as consecutive dendronization or thickening, the molar mass of the starting polymer **PG1** had to be carefully chosen. High molar masses may result in handling and characterization problems. The initial focus was therefore placed on a "short" **PG1** with $P_n \approx 1000$ and $L \approx 250$ nm. Assuming complete coverage throughout, its corresponding **PG4** had a molar mass of approximately 5.5 ×

(24) A theoretical study predicts persistence lengths λ of third and fourth generation dendronized polymers to be 50 and 120 nm, respectively, and lead to the "Janus chain" model for dendronized polymers: (a) Ding, Y.; Öttinger, H. C.; Schlüter, A. D.; Kröger, M. *J. Chem. Phys.* **2007**, *127*, 094904. Kröger, M.; Peleg, O.; Ding, Y.; Rabin, Y. *Soft Matter* **2008**, *4*, 18–28. Ding, Y.; Kröger, M. *Macromolecules* **2009**, *42*, 576–579. For λ of dendronized polymers up to generation three determined by SANS, see: (b) Stocker, W.; Schürmann, B. L.; Rabe, J. P.; Förster, S.; Lindner, P.; Neubert, I.; Schlüter, A. D. *Adv. Mater.* **1998**, *10*, 793–797. (c) Förster, S.; Neubert, I.; Schlüter, A. D.; Lindner, P. *Macromolecules* **1999**, *32*, 4043–4049. A comprehensive LS and SANS study on homologous series of dendronized polymers is presently being performed: (d) Sigel, R.; Guo, Y.; Zhang, A.; Schlüter, A. D.; Schurtenberger, P. In preparation. For λ of dendronized polymers up to the fifth generation determined by MALLS, see: (e) Percec, V.; Ahn, C.-H.; Cho, W. D.; Jamieson, A. M.; Kim, J.; Leman, T.; Schmidt, M.; Gerle, M.; Möller, M.; Prokhorova, S. A.; Sheiko, S. S.; Cheng, S. Z. D.; Zhang, A.; Ungar, G.; Yeardley, D. J. P. *J. Am. Chem. Soc.* **1998**, *120*, 8619–8631. (f) Ouali, N.; Mèry, S.; Skoulios, A.; Noirez, L. *Macromolecules* **2000**, *33*, 6185–6193. See also ref 6e.

(25) Costa, L. I.; Kasemi, E.; Storti, G.; Morbidelli, M.; Walde, P.; Schlüter, A. D. *Macromol. Rapid Commun.* **2008**, *29*, 1609–1613.

(26) In certain special cases mixed strategies may be feasible alternatives as well.

(27) For studies in which structural defects were quantified by either UV- and fluorescence spectroscopic or NMR-spectroscopic analysis, see refs 6d, f and 6g.

(28) Reference 6e does not provide information on the quantity in which these polymers were synthesized.

(29) Canilho, N.; Kasemi, E.; Mezzenga, R.; Schlüter, A. D. *J. Am. Chem. Soc.* **2006**, *128*, 13998–13999.

(30) For example, see Shu, L.; Schlüter, A. D.; Ecker, C.; Severin, N.; Rabe, J. P. *Angew. Chem., Int. Ed.* **2001**, *40*, 4666–4669.

Scheme 1. Attach-to Route to a Strictly Homologous Series of First through Fourth Generation Dendronized Polymers **PG1**−**PG4** and Structures of Compounds **2a** and **2b**, **Mg2**, and **3a** and **3b**[a]

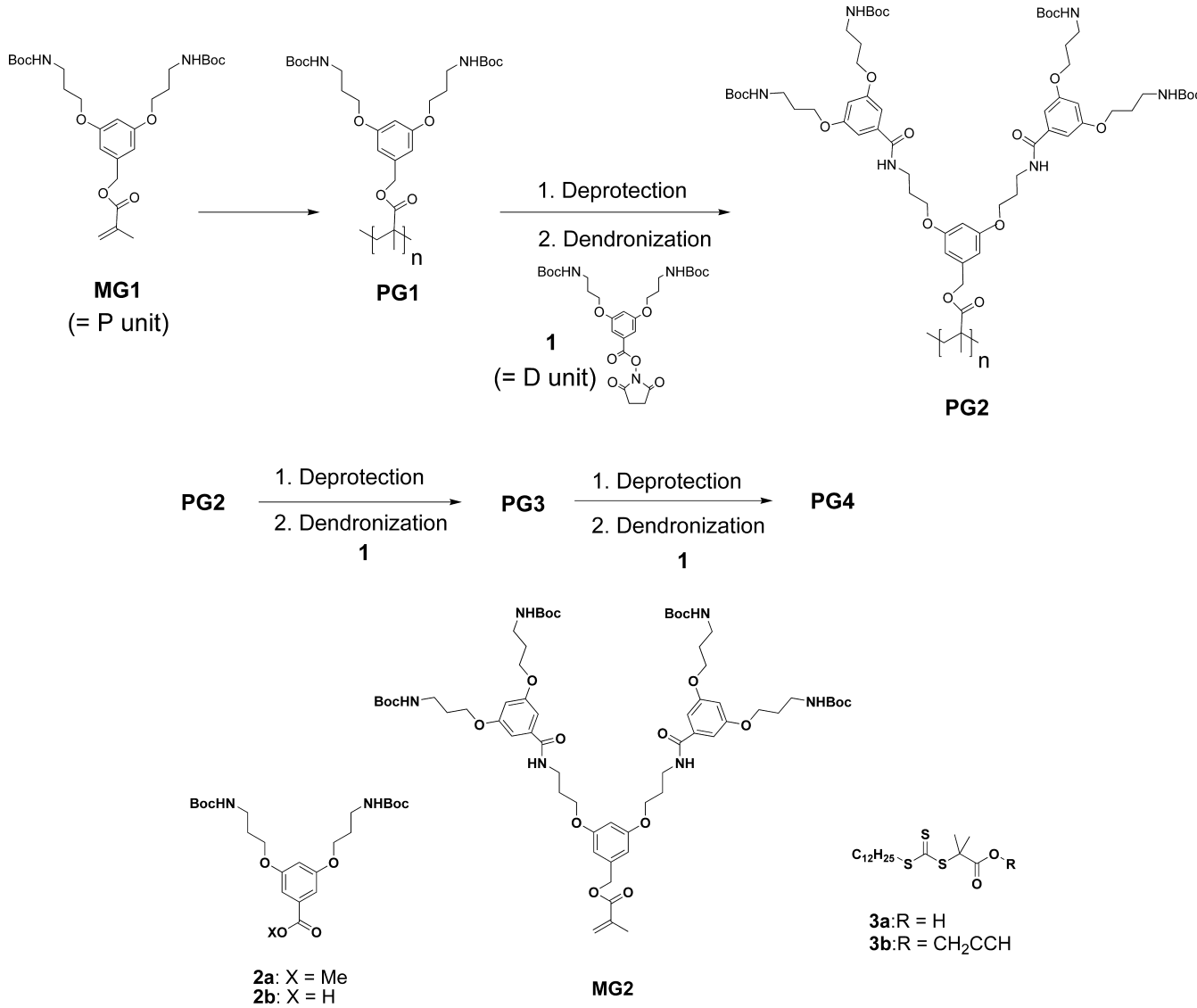

[a] Boc stands for *tert*-butyloxycarbonyl, a common protecting group for amine functional groups. Dendron **1** serves as the key building block to increase *g*.

10^6. With our experience such a **PG4** was expected to be soluble in organic solvents at room temperature and still exhibit sufficiently resolved NMR spectra. It was therefore considered a "safe" series. A longer and potentially more interesting series starting from a **PG1** with $L > 1$ μm was also planned. This of course involved the risk of lower solubility and complicated structural analysis especially for higher generation polymers. In order to synthesize these two **PG1**'s of different length both reversible addition−fragmentation chain transfer polymerization (RAFT)[31] and free radical polymerization (FRP) of **MG1** suggested themselves.

The main characterization effort involved methods providing *qualitative* insights concerning the growth processes. These methods comprised gel permeation chromatography (GPC), ^{13}C NMR spectroscopy, and atomic force microscopy (AFM) apparent height measurements. To be on the safe side all the samples were also checked by a *quantitative* method based on UV absorption. In it the unreacted terminal amines of the dendronized polymers were converted into UV labels with high extinction coefficient by reacting them with an excess of Sanger reagent (see Supporting Information).[6d] Finally, the NMR spectra of the second generation polymers obtained by the attach-to route were compared to those obtained by the macromonomer route starting from **MG2** (Scheme 1). This latter polymer is referred to as **PG2M**.

III.b. Synthesis and Structure Analysis. FRP of **MG1** has already been reported.[29] It was typically carried out on a 500 mg scale and yielded extremely high molar mass products. For the present work this scale was considered too low and polymerizations were done with up to 8 g of monomer per batch. Whereas **PG1** obtained from smaller scale experiments showed monomodal distributions with a polydispersity index PDI = 3−4, the present scale gave products with number average molar

(31) (a) Chiefari, J.; Chong, Y. K.; Ercole, F.; Krstina, J.; Jeffery, J.; Le, T. P. T.; Mayadunne, R. T. A.; Meijs, G. F.; Moad, C. L.; Moad, G.; Rizzardo, E.; Thang, S. H *Macromolecules* **1998**, *31*, 5559–5562. For a review, see: (b) Barner-Kowollik, C.; Davis, T. P.; Heuts, J. P. A.; Stenzel, M. H.; Vana, P.; Whittaker, M. *J. Polym. Sci. Polym. Chem. Ed.* **2003**, *41*, 365–375. For an application to dendronized polymers, see: (c) Zhang, A.; Wei, L.; Schlüter, A. D. *Macromol. Rapid Commun.* **2004**, *25*, 798–803.

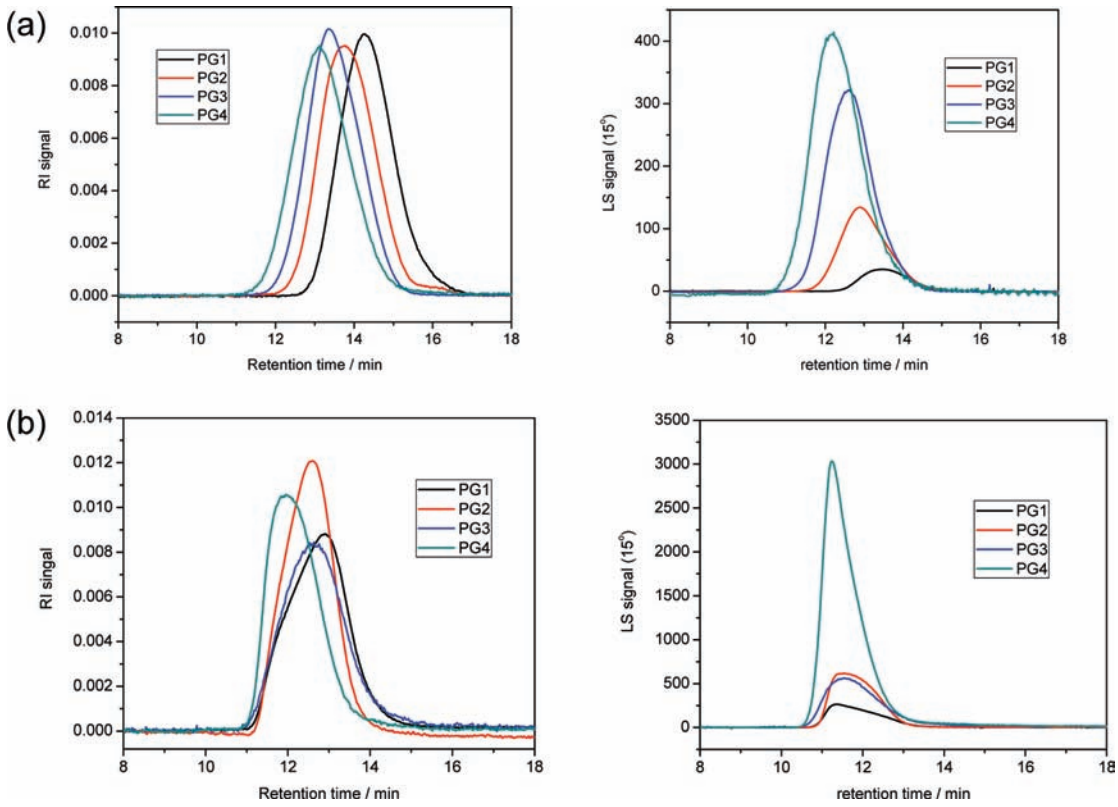

Figure 5. GPC elution curves based on refractive index (left) and Light Scattering (LS) detection at 15° scattering angle (right) of the homologous series (a) $\mathbf{PG1_{1000}}$−$\mathbf{PG4_{1000}}$ and (b) $\mathbf{PG1_{7000}}$-$\mathbf{PG4_{7000}}$. All elution curves of one set belong to one and the same homologous series. All measurements were done in DMF (1% LiBr) at 45 °C.

masses in the range of $M_n < 1 \times 10^6$ and a rather broad PDI ≈ 6.5. Fractionating precipitation of the 5.8 g of raw **PG1**[29] obtained yielded two fractions with $M_n \approx 6.2 \times 10^6$ (1.6 g) and $M_n \approx 3.6 \times 10^6$ (1.5 g); the remaining broadly distributed material amounted to 2.7 g. The second fraction, whose elution curve is shown in Figure 5 contained chains with $P_n \approx 6800$ (PDI = 1.9) and was used as starting material for the high molar mass series, hereafter referred to as $\mathbf{PG1_{7000}}$. The shorter chain **PG1** was obtained using the RAFT reagent **3b** (Scheme 1), which was synthesized from the corresponding carboxylic acid **3a**[32] by standard esterification. The polymerization was done at 60 °C with AIBN as initiator and gave a **PG1** with $M_n \approx 0.5 \times 10^6$ and PDI = 1.4 in a yield of 83%. This sample had $P_n \approx 1000$ by GPC and was used as starting material for the low molar mass series, hereafter referred to as $\mathbf{PG1_{1000}}$. Its GPC elution curve is also contained in Figure 5. All dendronizations were performed in DMF with an excess of the active ester dendron **1**, which was obtained from the corresponding acid **2**[6a] on a 200 g scale by standard chemistry. It was critical to add compound **1** in portions and to lower the temperature before each addition from 20 to −5 °C. All synthetic operations are detailed in the Experimental (see SI). Most of the data from combustion analysis are within the expected range showing that the polymers do not act as a "sponge" for solvents or impurities (see Supporting Information, Table S1, for the $\mathbf{PG_{7000}}$ series).

The way the freeze-drying and deprotection procedures were carried out turned out to be especially important for maximizing the coverage. Before each synthetic step both the protected and deprotected polymers were freeze-dried from dioxane and water, respectively, observing an initial concentration of 2 g of polymer in 20−30 mL solvent. Though the procedures required a couple of days, the materials obtained had a very fine, foam-like morphology. Samples that easily flew upon friction induced electrostatic charging were considered of sufficient quality. If the mixtures happened to partially melt during the process, the products were sticky and freeze-drying was repeated. Deprotections were typically done on the 2 g scale in neat trifluoroacetic acid. The reactions were quenched with MeOH by which the acid was converted into the more volatile corresponding methylester. A second portion of MeOH was always added to remove the last traces of residual trifluoroacetic acid as the corresponding ester during freeze-drying (see Experimental). The completion of deprotection was confirmed prior to the next step by rigorously applied NMR spectroscopy showing the disappearance of the *tert*.-butyl signal at $\delta = 1.38$ ppm.

The synthesis conditions and results for $\mathbf{PG1_{1000}}$ and $\mathbf{PG1_{7000}}$ are compiled in Table 2. For the shorter series, the yields of isolated products were essentially constant and above 80% for each step, whereas for the longer series they decreased from 80% for $\mathbf{PG2_{7000}}$ to 70% for the two higher homologues. These numbers refer to freeze-dried, ready to use samples and are considered optimized. The yields observed can neither be correlated with the achieved degree of coverage nor do they give insight into whether or not inadvertent fractionation has taken place during chromatographic purification. High molar mass chains may adhere preferentially to the column support material. The possibility that insufficient coverage affects the yields was addressed by determining the degrees of coverage by the published method,[6d] using the same reference compound. This was ruled out because the coverage was virtually quantitative in all cases (see below).

(32) Lai, J. T.; Filla, D.; Shea, R. *Macromolecules* **2002**, *35*, 6754–6756.

Table 2. Synthesis Conditions and Results for $\mathbf{PG_{1000}}$ and $\mathbf{PG_{7000}}$

		PG1[a]	PG2[b]	PG3[c]	PG4[d]
Short series	Yield(%)	83	85	85	82
	P_n[e]	1000	950	1000	1300
	PDI	1.4	1.5	1.6	1.7
	T_g (°C)	45	66	75	73
Long series	Yield(%)	97	80	70	70
	P_n[e]	6800	6700	6400	6300
	PDI	1.9	1.6	1.8	1.7
	T_g (°C)	50	66	71	72

[a] P_n = 7000: fractionated from **PG1** ($M_n = 8.8 \times 10^4$, PDI = 6.5); P_n = 1000: [**MG1**]/[**7**]/[AIBN] = 1200/1/0.5 in dry DMF at 60 °C for 24 h. [b] [*de*-**PG1**]/[**1**] = 1/10 in dry DMF at −5 °C for 5 d. [c] [*de*-**PG2**]/[**1**] = 1/20 in dry DMF at −5 °C for 10 d. [d] [d] [*de*-**PG3**]/[**1**] = 1/40 in dry DMF at −5 °C for 20 d. [e] [e] Based on GPC in DMF (1% LiBr) at 45 °C using LS detection.

The glass transition temperatures T_g are in the expected range which is well below that of parent PMMA (T_g = 105 °C). They are obviously not dominated by the main chain but rather by the dendrons.[33] The T_g's were compared within the $N = 1000$ and $N = 7000$ series. In addition, for **PG2** and **PG3** they were also compared with $\mathbf{PG2_M}$ and $\mathbf{PG3_M}$.[34] Whereas both $\mathbf{PG2_{1000}}$ and $\mathbf{PG2_{7000}}$ have the transition at the same temperature, T_g = 66 °C, $\mathbf{PG2_M}$ has T_g = 67 °C. The third generation polymers $\mathbf{PG3_{1000}}$ and $\mathbf{PG3_{7000}}$ have slightly differing values of T_g = 75 and 71 °C, respectively, while the corresponding $\mathbf{PG3_M}$ has T_g = 73 °C. $\mathbf{PG4_{1000}}$ and $\mathbf{PG4_{7000}}$ have again virtually identical transitions with T_g = 75 and 71 °C, respectively. The fact that the T_g's of these two **PG4**'s do not occur at higher temperatures than that of the **PG3**'s has precedents.[33] Large structural defects are intuitively expected to result in larger differences of T_g.

The GPC elution curves for the $\mathbf{PG1_{7000}}$−$\mathbf{PG4_{7000}}$ series are shown in Figure 5. Note that for the long series the available PMMA standard did not cover the entire calibration range giving rise to uncertainty regarding the P_n values. The molar masses are based on refractive index and single angle light scattering detection (15°). For both series the elution volumes decrease with increasing side chain generation. This is qualitatively expected, because the chain stiffness increases with the dendron generation leading to a larger hydrodynamic volume. At the same time the molar mass for a given degree of polymerization increases dramatically, as reflected in the strongly increasing peak area for the light scattering signal. The elution curves for the shorter series are strictly monomodal.[6e] It is well-known although not understood in detail that an anomalous elution behavior might be observed for particularly large polymer structures with complex chain topologies, such that the longest chains are retarded and coelute with much shorter ones.[35,36] Such an effect is visible in the elugrams of the $\mathbf{PG_{7000}}$ series causing peculiar and strongly varying shapes of the elution curves. This effect depends on the injection concentration, the adsorption tendency onto the column material and other subtle factors. Anomalous elution falsifies the determination of PDI and the universal calibration results. However, it does not prohibit the correct determination of M_w, provided that concentration losses can be avoided. The latter becomes apparent in the peak area of the RI-detector normalized by the injection concentration which is shown in Figure 5.

Next, NMR spectroscopy was used to investigate coverage. First it was shown for the $\mathbf{PG1_{7000}}$ series that the intensity of the backbone signals decreases relative to the signals of the dendritic shell, when the generation increases. In order to avoid insurmountable problems with extreme line widths we utilize ^{13}C NMR spectroscopy in the solid state rather than ^{1}H NMR spectroscopy in solution. This was done despite the fact that all samples, contrary to our initial expectations, dissolved reasonably quickly and completely (by visual inspection) in common organic solvents like chloroform, dichloromethane, THF and DMF at room temperature. Figure 6 compares the relevant spectra which were normalized to dendron signals and shows that the intensities of the backbone signals (marked by arrows) decrease continuously. These spectra were also used to extract information about the local order of the dendrons in the four different polymers. Since the line widths of all dendritic carbons were basically the same (3−5 ppm) the local order is likely to be the same for all polymers.

Second, the polymers $\mathbf{PG2_{7000}}$ and $\mathbf{PG2_M}$ which had been prepared by the attach-to and macromonomer routes, respectively, were directly compared by ^{1}H and ^{13}C NMR spectroscopy (Figure 7). Both pairs of spectra are almost superimposable. This suggests high coverage. It should be noted though that the $\mathbf{PG1_M}$ and $\mathbf{PG1_{7000}}$ polymers may differ in their backbone stereochemistry because of the different steric requirements of the dendritic substituents **MG1** and **MG2**. **MG1** determines the backbone stereochemistry in $\mathbf{PG2_{7000}}$ and **MG2** the one of $\mathbf{PG2_M}$.[37] By inspection of the region between $\delta = 0.8-1.2$ ppm in spectra a and b (Figure 7), it can be concluded that both polymers are mainly atactic with $\mathbf{PG2_{7000}}$ having a somewhat higher syndiotactic content.[38] The respective NMR spectra were therefore not expected to be superimposable in every detail.

Further, the chain thickening process was visualized by atomic force microscopy (AFM). Equal parts of dilute chloroform solutions of the four polymers $\mathbf{PG1_{1000}}$−$\mathbf{PG4_{1000}}$ were combined and the resulting solution spin-coated onto mica. The dry samples were imaged in tapping mode (Figure 8a). All chains, even in larger scale images showing hundreds of them, could unambiguously be classed into four categories assigned as **PG1**−**PG4**. Having imaged the four kinds of chains under identical conditions allowed to determine their apparent heights using an automated method recently developed by one of the authors (M.K.).[39] This method identifies chains which are not involved in aggregates or contain other nonanalyzable parts and determines the height profile along the contour. A typical height profile for an individual $\mathbf{PG4_{1000}}$ chain is shown in Figure 8b, whose inset indicates how the center-line was obtained. All height profiles fluctuate. This may be due to several reasons such as the occurrence of kinetically trapped, frozen-in conformations, secondary structure formation (e.g., helices), and structural defects stemming from synthesis. The average apparent height was determined from the height profile of each

(33) For the glass transition temperatures of closely related polymers made by the macromonomer route, see:Zhang, A.; Okrasa, L.; Pakula, T.; Schlüter, A. D. *J. Am. Chem. Soc.* **2004**, *126*, 6658–6666.
(34) Kasemi, E.; Schlüter, A. D. unpublished.
(35) This material showed an anomalous elution behavior resulting in a multimodel elution curve. This may in part be caused by high molar mass chains eluting at unusually high retention times because of interaction with the support.
(36) (a) Wintermantel, M.; Antonietti, M. J; Schmidt, *J. Appl. Polym. Sci., Polym. Symp.* **1993**, *52*, 91. (b) Gerle, M.; Fischer, K.; Müller, A. H. E.; Schmidt, M.; Sheiko, S. S.; Prokhorova, S.; Möller, M. *Macromolecules* **1999**, *32*, 2629.
(37) For a recent related case, see Zhang, A.; Rodriguez-Ropero, F.; Zanuy, D.; Alemán, C.; Meijer, E. W.; Schlüter, A. D. *Chem.—Eur. J.* **2008**, *14*, 6924–6934.
(38) Hatada, K.; Kitayama, T.; Ute, K. *Prog. Polym. Sci.* **1988**, *13*, 189–276.
(39) http://www.complexfluids.ethz.ch/polymerAFM.

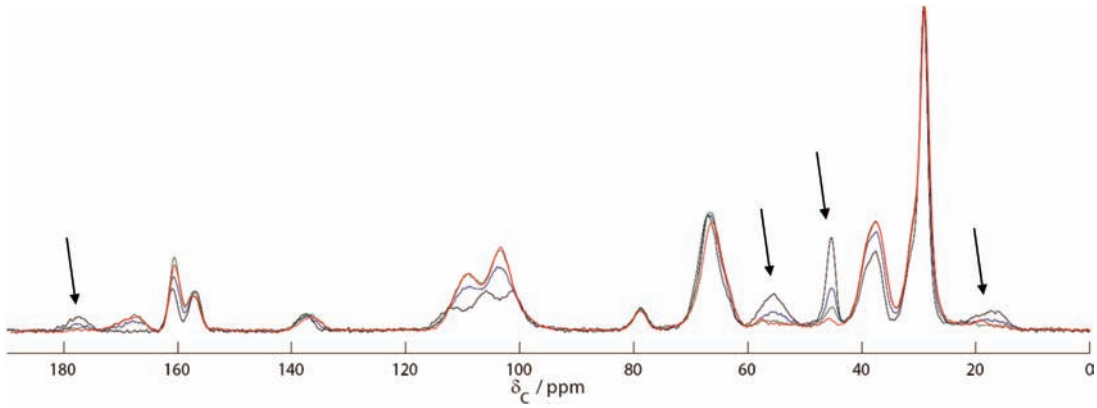

Figure 6. CPMAS ^{13}C NMR spectra of $\mathbf{PG1}_{7000}$–$\mathbf{PG4}_{7000}$. Note that the signals marked with arrows belong to the backbone. Their intensity decreases systematically with increasing generation which is especially clear for the signal at approximately $\delta = 45$ ppm. Color code: black, **PG1**; blue, **PG2**; green, **PG3**; red, **PG4**.

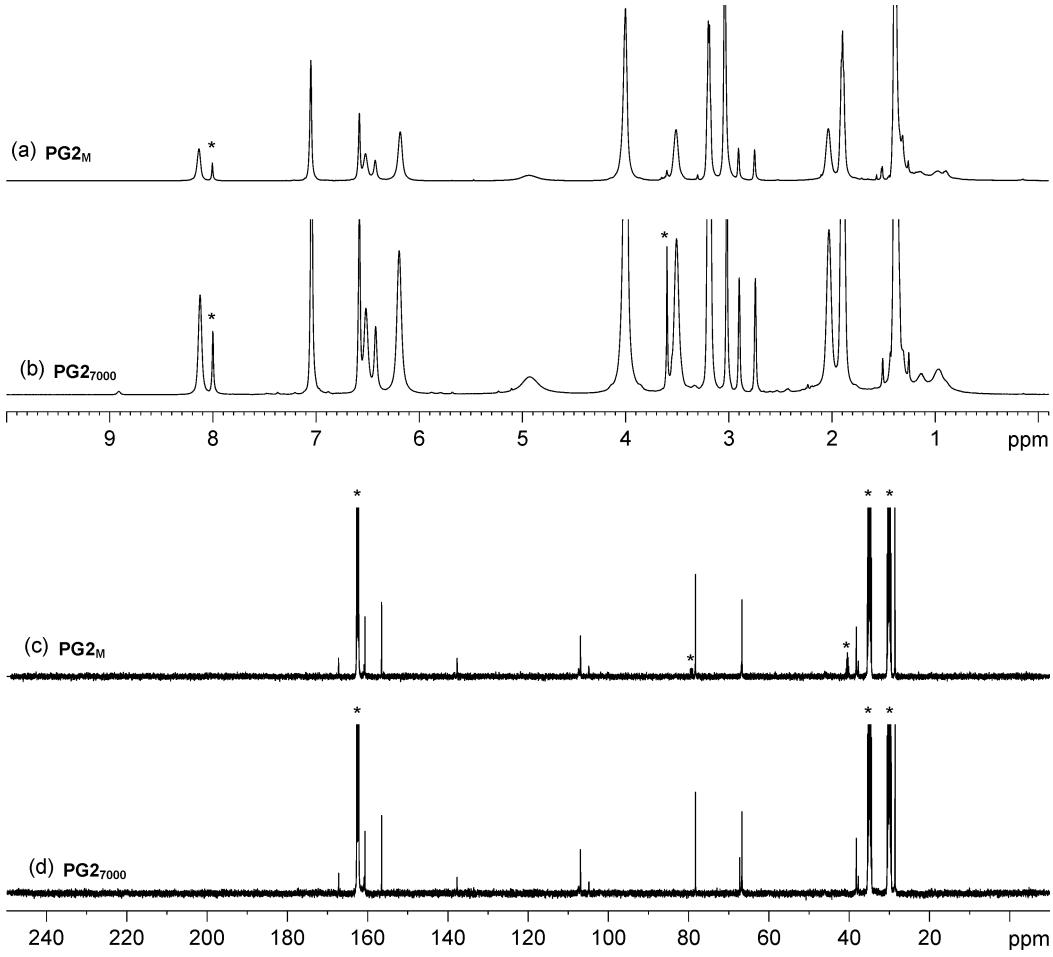

Figure 7. NMR spectral comparison of polymers **PG2** synthesized according the macromonomer route, $\mathbf{PG2}_{M}$ and attach-to route, $\mathbf{PG2}_{7000}$: ^{1}H NMR spectra of $\mathbf{PG2}_{M}$ (a) and $\mathbf{PG2}_{7000}$(b); ^{13}C NMR spectra of $\mathbf{PG2}_{M}$ (c) and $\mathbf{PG2}_{7000}$ (d). The ^{13}C NMR spectra were recorded at the highest possible concentration and accumulating 20000 pulses. Solvent signals (DMF-d_7, $CDCl_3$) are marked (*). The signal in the ^{13}C NMR spectrum of $\mathbf{PG2}_{7000}$ at $\delta = 67$ ppm stems from residual dioxane, the solvent used for freeze-drying.

polymer. The resulting average values of a statistically significant ensemble of chains of different generations were then again averaged. The plot of the resulting apparent height values against generation is depicted in Figure 8c. The chain heights increase by approximately 8.5 Å per generation, assuming the interaction between tip and polymer is identical for all generations. Because the side chain dendrons all have the same repeat units and the same terminal units this assumption is reasonable. However, for the low generation polymers, the polymer–substrate interactions are expected to differ and may result in different cross-sectional shapes. The linear correlation in Figure 8c may thus be accidental. The chain height increase was also measured for the long series $\mathbf{PG1}_{7000}$–$\mathbf{PG4}_{7000}$ and found to be identical. A representative AFM image can be found in the Supporting Information. Similarly, a "persistence length" of the adsorbed chain has been directly obtained from the tangent–tangent

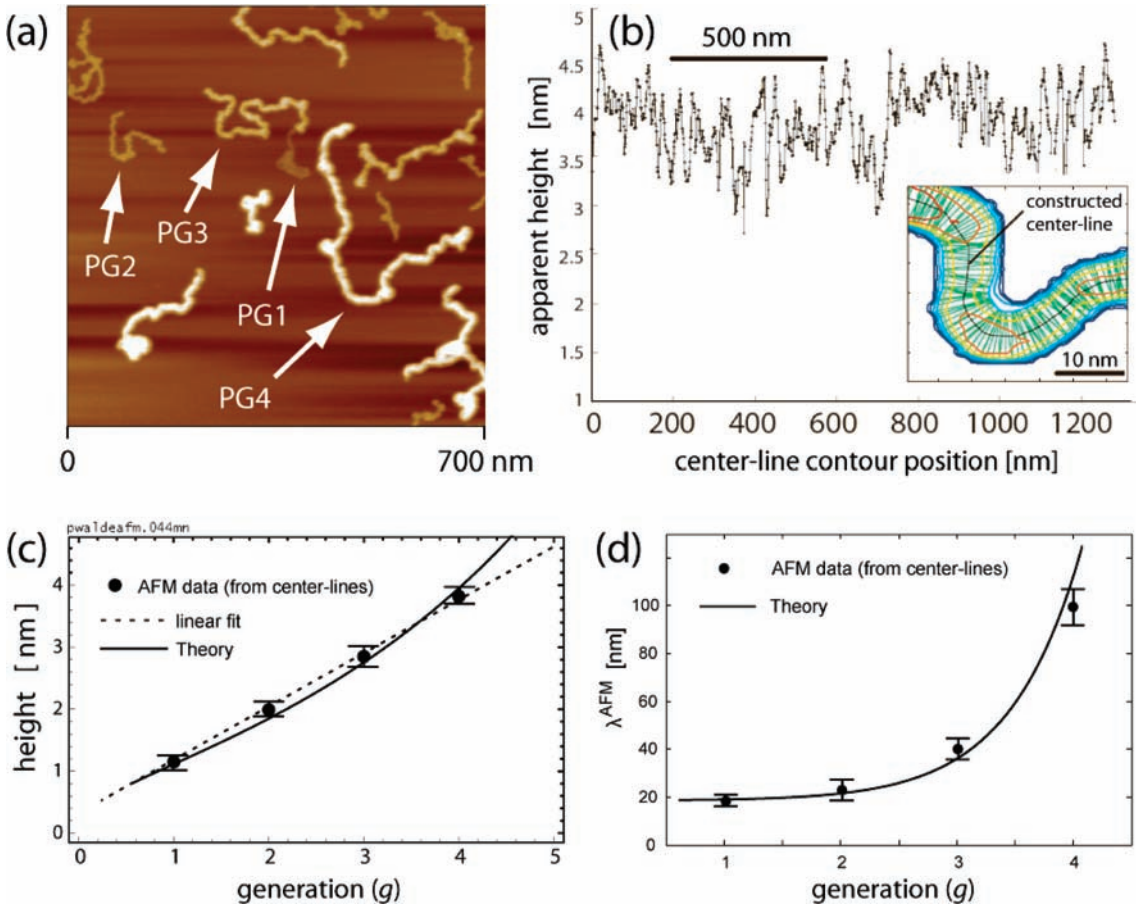

Figure 8. (a) AFM height image of a mixture of $\mathbf{PG1}_{1000}-\mathbf{PG4}_{1000}$ spin-coated from chloroform onto mica showing mainly individual entities. Representative chains of each generation are marked. For data collection and analysis larger images (1.5 μm x 1.5 μm) were used. (b) Determination of an apparent height profile of a $\mathbf{PG4}_{1000}$ chain using a tool that recognizes chains and their closed envelopes, thus ignores the background, and allows studying height profiles of single chains, like the one shown, in detail (see ref 39). The inset is a zoom into the contour plot of a region of a dendronized polymer. Lines generally follow equidistant heights. The green lines, however, are perpendicular to the center-line and are calculated by searching for spatially nearest neighbors on same contour lines, separated by at least one-third of the size of the whole polymeric object. The "center-line" connects adjacent middle points of the green lines. Its coordinates allow extracting heights along the centerline. (c) Apparent heights of $\mathbf{PG1}_{1000}-\mathbf{PG4}_{1000}$ versus generation. The straight dotted line is a least-squares linear fit. Since the AFM measurements were carried out in the air, on dry samples, the thickness of the chains is expected to correspond to the collapsed state of the side chains when $r^2\delta \approx \upsilon_{\text{monomer}} n$ leading in the case of $X = 3$ to $r \approx (\upsilon_{\text{monomer}}/\delta)^{1/2}(2^g - 1)^{1/2}$(solid line). For the range considered this expression is close to the observed linear dependence though deviations are expected at higher generations. (d) "AFM persistence length" of the adsorbed chains versus generation. Solid line is using eq 11.

correlation of the center-line at separations larger than the length scale of the local undulations. This quantity is shown in Figure 8d. The stiffness clearly increases with number of generations, as predicted by eq 11. Yet, this agreement should be considered with caution and may be accidental because eq 11 describes the behavior of free chains in good solvent while the AFM data corresponds to adsorbed chains in a dry state. It turns out that the center-lines of the adsorbed dendronized polymers do not exhibit wormlike chain statistics, which we attribute to the effect of the adsorption process.

As noted above, the structural fidelity of both series was also investigated using a UV labeling technique. For details and the impact of the nature of the reference compound, see Supporting Information. For a discussion of the limits of the method, the reader is referred to the original paper.[6d] The following results were obtained for $\mathbf{PG2}_{1000}-\mathbf{PG4}_{1000}$: 99.8, 99.8, and 99.7%, respectively, and for $\mathbf{PG2}_{7000}-\mathbf{PG4}_{7000}$: 99.8, 99.7, and 99.3%, respectively. While the coverage decreases with increasing generation and increasing chain length, it is nevertheless virtually quantitative.

We explored the synthesis of larger quantities of the $N \approx 1000$ series. Our initial starting point involved 6 g of *de*-$\mathbf{PG1}_{1200}$ (the prefix *de* indicates deprotected), a starting material independently prepared form the above series. With the same procedure as described above the yield for **PG2** was only about 65%. To improve this low yield we divided the starting polymer into 2 g batches which were combined after parallel dendronization. The combined yield of this procedure could be raised to 90% and the largest amount of $\mathbf{PG2}_{1200}$ which was prepared this way was 12 g. This splitting and combining technique was repeated for the remaining two generations to provide these materials in yields of approximately 80%. The combined samples of $\mathbf{PG3}_{1200}$ and $\mathbf{PG4}_{1200}$ amounted to 8 g in both cases.

IV. Discussion

Comparison between theory and synthesis reveals two issues. One concerns the applicability range of the theory. The second concerns the solvent quality of the dendronized polymers. The simple theory represented applies to dendrons whose strands exhibit Gaussian elasticity. In turn this imposes constraints on the polymers considered. In the absence of spacer chains the theory begins to apply roughly at $g = 4$. Accordingly the minimal series allowing to probe the scaling behavior predicted

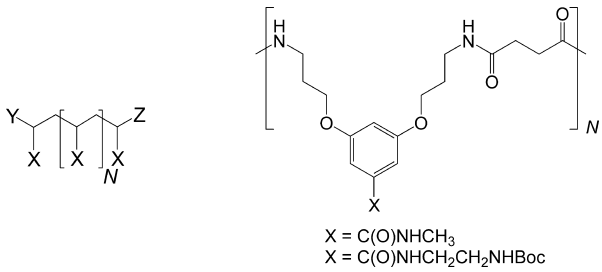

Figure 9. Linear homopolymer comprising either free dendron ends and interior dendron units or just interior dendron units depending on choice of X (left). Possible realizations (right).

should incorporate $g = 4-6$. When the dendronization monomers incorporate long spacer chains the scaling regime is wider beginning at $g = 1$. This last architecture also affords the advantage of postponing the closed packing limit to higher g values. Preliminary results suggest $g = 5-6$ can be attained with current "spacer less" chemistry.[40] One should note that synthetic schemes involving long spacer chains have been reported thus suggesting that homologous series with $g = 1-5$ are feasible.[41] Monomers with $X = 4$ were also reported.[42]

A second, more insidious problem concerns solvent quality. Our theoretical analysis focused on the case when free ends and interior monomer in the dendron experienced identical good solvent conditions and identical monomer monomer interactions. This assumption was invoked to allow for a brief discussion of molecular design parameters and their roles. The generalization of this picture is straightforward. It incurs however the price of introducing additional interaction parameters characterizing the solvent quality experienced by free ends and the interior monomers as well as their mutual interactions. Since the fraction of free ends is larger than 50%, their role is never negligible and confrontation of theory with experiment requires characterization of the individual interaction parameters. In turn this requires a synthetic effort to create linear homopolymers comprising of monomers similar to the free ends or to the interior units and Figure 9 offers concrete suggestions.

By choosing X = $C(O)NHCH_3$ a homopolymer is obtained comprising the interior units of the dendrons and for X = $C(O)NHCH_2CH_2NHBoc$ the chains obtained consist of repeat units corresponding each to a dendritic free end. The solubility and swelling behavior of such polymers will allow specifying the necessary parameters. With these parameters at hand one may reformulate the theory so as to capture the swelling regime of the side chains. A similar approach was explored by Hawker et al. who synthesized linear analogs of dendrimers.[43] The lower solubility of the linear chains was attributed to their high propensity to crystallization.

V. Summary and Outlook

The synthetic method announced affords two advantages (i) gram scale yields, (ii) dendronized polymers with extremely monodisperse dendrons even in the case where 56 000 dendronization reactions are performed per macromolecule as in the case of converting $\mathbf{PG3_{7000}}$ to $\mathbf{PG4_{7000}}$. In addition, this method appears to be a generally applicable dendronization tool for chains carrying amine groups. This approach allows tuning the thickness of short as well as long polymers.

The combination of the theory and the synthesis results suggests that the scaling behavior of dendronized polymers can be explored in the foreseeable future. It requires however further synthetic effort to create dendronized polymers in the scaling regime and linear homopolymers designed to characterize the different interaction parameters involving free ends and interior monomers.

Acknowledgment. This work was supported by ETH research grants TH-1608-1 and TH-0908-2 as well as by EU-NSF contract NMP3-CT-2005-016375 and FP6-2004-NMP-TI-4 STRP 033339 of the European Community. The authors thank Dr. R. Sigel, University Fribourg, for helpful comments and are indebted to Profs. A. Vasella, M. Textor, and N. Spencer (all ETH) for generously providing access to their equipment. The authors cordially thank Prof. Manfred Schmidt for constructive discussions.

Supporting Information Available: All synthetic procedures and analytical data. Determination of coverage. AFM image of coprepared samples of $\mathbf{PG1_{7000}}-\mathbf{PG4_{7000}}$. This material is available free of charge via the Internet at http://pubs.acs.org.

JA9032132

(40) Zhang, B.; Kröger, M.; Halperin, A.; Schlüter, A. D. In preparation.
(41) For dendronized polymers with varied spacer lengths, see: Li, W.; Zhang, A.; Schlüter, A. D. *Chem. Commun.* **2008**, *552*, 3–5525. Li, W.; Zhang, A.; Feldman, K.; Walde, P.; Schlüter, A. D. *Macromolecules* **2008**, *41*, 3659–3667.
(42) Buchowicz, M. N.; Holerca, V.; Percec, V. *Macromolecules* **2001**, *34*, 3842–3848. Bao, Z.; Amundson, K. R.; Lovinger, A. J. *Macromolecules* **1998**, *31*, 8647–8649.
(43) Hawker, C. J.; Malmström, E. E.; Frank, C. W.; Kampf, J. P. *J. Am. Chem. Soc.* **1997**, *119*, 9903–9904.